https://doi.org/10.20965/jrm.2010.p0348

Paper:

Development of a Robot Balanced on a Ball – First Report, Implementation of the Robot and Basic Control –

Masaaki Kumagai* **and Takaya Ochiai****

*Tohoku Gakuin University
E-mail: kumagai@tjcc.tohoku-gakuin.ac.jp
**Graduate school, Tohoku Gakuin University

[Received September 29, 2009; accepted March 3, 2010]

This paper proposes the implementation and control scheme of a robot balanced on a ball. Unlike a two-wheeled inverted pendulum, such as the Segway Human Transporter, an inverted pendulum using a ball moves in any direction without changing orientation, enabling isotropic movement and stabilization. The robot on the ball can be used in place of the two-wheeled robots. Our robot has three omnidirectional wheels with stepping motors that drive the ball and two sets of rate gyroscopes and accelerometers as attitude sensors. It can keep station, traverse in any direction, and turn around its vertical axis. Inverted pendulum control is applied to two axes to maintain attitude. Ball acceleration is used as control input of the system, unlike most of inverted pendulums which use torque or force as input. This acceleration input makes the robot robust against change of inertia parameters, as confirmed by Nyquist diagrams. The mechanism of the robot, the control method, and the experimental results are described in this paper.

Keywords: inverted pendulum, ball balance, stepping motor, omnidirectional wheel, ballbot

1. Introduction

The ball-riding robot we developed to ride and balance on a ball was inspired by acrobatic human and animal feats such as those commonly seen at the circus. *BallIP*, as we call it, was realized using the inverted pendulum control and an omnidirectional driving mechanism for the ball.[1]

We have developed several types of pendulums, including a wheel-driven pendulum that could ride on a pipe as shown in **Fig. 1(a)**. It was a prototype robot, whose concept has been applied to the proposed robot. In addition, many of omnidirectional mobile robots were informative in ball drives.

There were previous efforts on such robots. Many inverted pendulums have been developed for mobility or as platforms to verify control algorithms. Practical applications such as the *Segway Human Transporter* [5] and Hitachi's *EMIEW* [6] are increasing, although they use wheels and have directional limitations in movement. However, an isotropic motion and thus isotropic stabilization or avoidance can be realized using a ball as a wheel.

Controlling a robot on a single ball using an inverted pendulum control had already been mentioned in the 1970s [7]. However, we know only a few successful robots.

The *ballbot* [8] of Lauwers et al. used an inverse mouse-ball drive for movement and a LQR control to feed back sensory information. The objective was a dynamically stable mobile robot tall enough to interact with human users. Although their first attempt did not rotate around the yaw axis due to drive limitations, they eventually added a yaw-drive to rotate the body [9].

B. B. Rider [10], a wheelchair proposed by Endo et al. used four omnidirectional drives for balancing on a ball and turning on a vertical axis. Unfortunately, to the best of our knowledge, practical results could not be found. Our concept using an omnidirectional ball drive and assuming the robot as an inverted pendulum is same to their work though we designed ours independently of their work. Our work differed from theirs mainly in realization, e.g., their torque control using a drive with four pairs of spherical wheels versus our acceleration control using a drive with three single-column omnidirectional wheels.

After developing a prototype pipe-riding robot, we focused on mobile robots using omnidirectional wheels such as that developed by Asama et al. [11, 12], which we selected because it remains in contact at a single point during wheel rotation rather than using two or more partially continuous trajectories.

2. Robot Mechanism

Following our first 1,300 mm tall prototype [3], we developed and built the 500 mm tall robot in **Fig. 1(b)**, which weighed 8.7 kg. We built four same robots for multi-robot experiments. The intended purpose of this robot was the transportation of loads, and it was designed to be shorter than the first prototype. This robot used bowling ball approximately 220 mm in diameter, weighing 3.8 kg, and coated in liquid rubber spray (Plasti Dip).

1. Parts of this paper have been presented at Robomec 08,09 [1, 2], ICCAS 08 [3], and ICRA 09 [4].

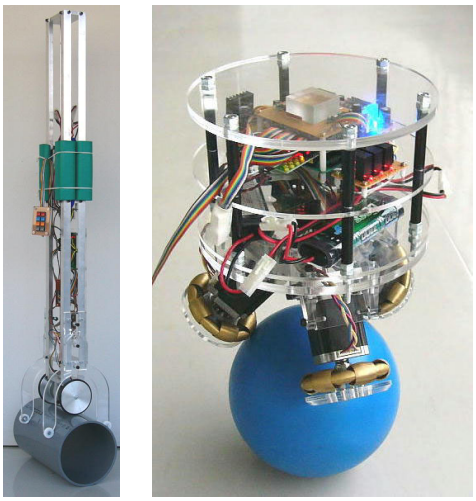

(a) pipe (b) ball

Fig. 1. Robots balancing on pipe and ball.

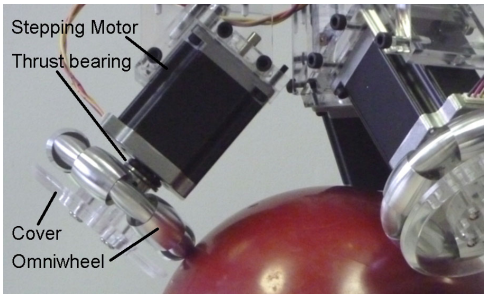

Fig. 2. Ball drive.

The mechanical properties of the ball were not measured, but it was not dented by the contact pressure of the wheels. It had enough friction between the wheels and the ball, and between the ball and a floor. A slip was observed when we tried to balance it on a slope of more than 8° inclination, where the motor also reaches the torque limit and begins to loose steps. The ball also slipped around the vertical axis when a large external torque was applied while the robot did not intend to turn.

The robot body consisted of an electronic circuits including sensors and a ball drive with three stepping motors and the omnidirectional wheels in **Fig. 2**. The wheel was directly attached to the shaft of the motor with no reduction gear, which reduced the mechanism backlash. The use of the stepping motors reduced the cost of the mechanism, the driving circuits, and the control software because of the stepping motor's open loop characteristics and its larger torque than that of a DC servomotor. This direct-drive mechanism provided a smooth and low oscillatory motion to the robot. Using stepping motors with an inverted pendulum is rare but not unheard of as shown by Hiraoka et al.'s focus on the advantages of stepping motors [13, 14].

As shown in **Fig. 3(b)**, the three wheels were fixed symmetrically at 120° intervals through the motor shaft to make them perpendicular to the tangent plane of the ball, as shown in **Fig. 3(c)**. Zenith angle ϕ was 50°. The omnidirectional wheel proposed by Asama et al. [11, 12] used for this robot has only one contact line, making it easy to drive the robot on a spherical surface. The wheel was 100 mm in diameter.

We used the unipolar motor KH56QM2–913 (Nidec Servo Co.) as a bipolar motor to obtain larger torque of approximately 2 Nm. Each motor had a microstep controller TA8435 (Toshiba semiconductor) to divide individual motor steps of 1.8°/step into 0.225°/step to smooth wheel rotation. Motors ran on three 7.2 V Ni-MH batteries, also used for the controller.

The control system used MEMS attitude sensors and a 16-bit micro-controller H8/3052 (Renesas). The output of two sets of an angular velocity rate gyro sensor ADXRS401 (Analog Devices) and an accelerometer ADXL203 (Analog Devices) are converted to inclination signals and combined into one inclination in frequency domain [15]. The rate gyro sensor signal is used for the higher response and that from the accelerometer for absolute inclination angle stability.

3. Robot Control

The robot was realized using an inverted pendulum control in two directions (back and forth and right and left) and an omnidirectional ball drive as mentioned above.

3.1. Robot Attitude and Station Control

Robot attitude and position (movement) are controlled separately in two orthogonal directions, simplified and modeled two-dimensionally as the wheeled inverted pendulum shown in **Fig. 4** having parameters listed in **Table 1**. The ball is assumed to be a *virtual* wheel controlled to maintain robot inclination θ at zero (vertical) and position x.

Figure 5 shows typical PD feedback control for our robot using the robot's inclination obtained by the sensors and the wheel's travel as follows:

$$\begin{aligned} a_x &= K_A\theta_x + K_{AV}\dot{\theta}_x + K_T(x - x_0) + K_V v_x \\ a_y &= K_A\theta_y + K_{AV}\dot{\theta}_y + K_T(y - y_0) + K_V v_y, \end{aligned} \quad \ldots \quad (1)$$

a is control input commanding *virtual* wheel acceleration, θ inclination toward each axis, x and y travel and v *virtual* wheel velocity. Subscripts x and y are related state variable axes and K the constant gains tuned experimentally. v and $x(y)$ were obtained by numerically integrating acceleration a. x, y, v_x, and v_y are measured on the ball rather than using world coordinates, i.e., $x = r\psi$. Although these values almost coincide with floor movement, a discrepancy is anticipated, especially if the robot's path is complex.

Kumagai applied the acceleration-input equation from the paper by T. Emura [7] to over 10 pendulums, including wheeled and reaction wheeled types. T. Emura mentioned in the paper the case that the control input to the system is the torque/force of the actuator as many of inverted pendulums do, while we had used the acceleration

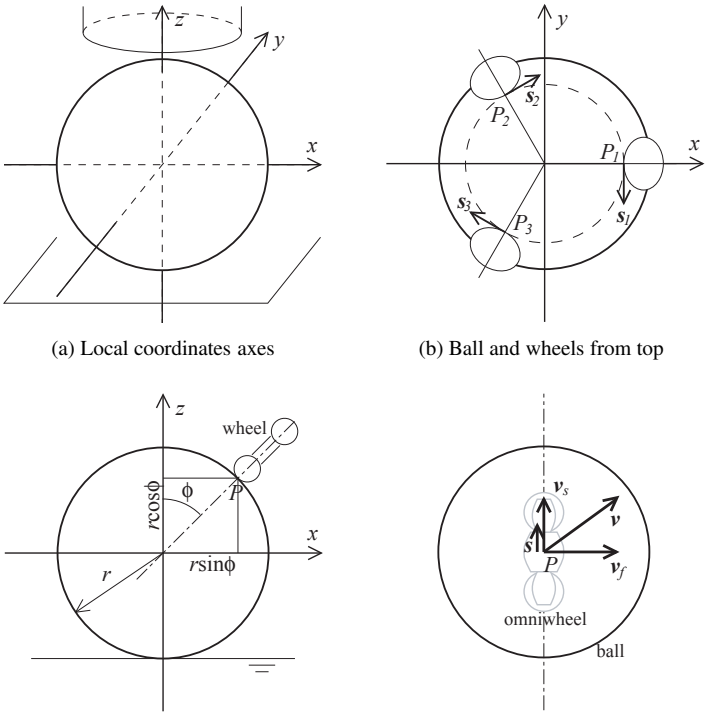

(a) Local coordinates axes (b) Ball and wheels from top

(c) Ball and wheel from side (d) Relative velocity between ball and wheel

Fig. 3. Axis definition and relationship between ball and wheels.

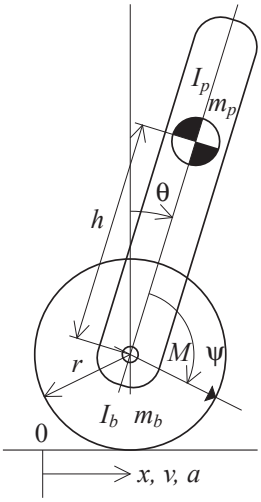

Fig. 4. Inverted pendulum model.

Table 1. Robot parameters.

m_p	Mass of robot	8.7	kg
I_p	Moment of inertia of robot	0.11	kgm^2
m_b	Mass of ball	3.8	kg
I_b	Moment of inertia of ball	0.018	kgm^2
r	Radius of ball	0.11	m
h	Height of center of mass	0.23	m

as the input, which was also suggested by T. Emura. The stability of the control was checked as that paper using the Hurwitz method, and also demonstrated using the Nyquist diagram as described later. We can also find several works

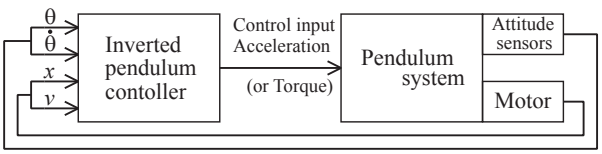

Fig. 5. Robot control block diagram.

using acceleration for the inverted pendulum [16].

We used the acceleration input to this robot because primarily we employed the stepping motor as the actuator. Some experimental results affected by disturbances showed that the acceleration input method is more robust than the torque input, whose detailed analysis is given later.

3.2. Wheel Speed Calculation for Ball Driving

As shown in **Fig. 3(a)**, we define a local coordinate frame with its origin at the ball center. Robot axes are fixed on the robot body, i.e., the z-axis is along the vertical line passing through the ball center and the robot's center of mass, and the x- and y-axes perpendicular to the z axis.

Wheel speed for acquiring the ball's angular velocity $\boldsymbol{\omega}$ is derived by letting the contact point between the wheel i and the ball be P_i, whose position vector is $\boldsymbol{p}_i$. Circumferential velocity $\boldsymbol{v}_i$ at P_i corresponding to the ball's angular velocity $\boldsymbol{\omega}$ is obtained as follows:

$$\boldsymbol{v}_i = \boldsymbol{\omega} \times \boldsymbol{p}_i. \quad \ldots\ldots\ldots\ldots\ldots\ldots \quad (2)$$

To derive the relationship between the ball's circum-

ferential velocity $\boldsymbol{v}$ and that of the wheel $\boldsymbol{v}_s$, as shown in **Fig. 3(d)**, speed $\boldsymbol{v}$ is resolved into components $\boldsymbol{v}_f$ parallel to the wheel axis and $\boldsymbol{v}_s$ perpendicular to it. $\boldsymbol{v}_f$ is generated by free rotation of wheel's small rollers and $\boldsymbol{v}_s$ the circumferential wheel speed. $\boldsymbol{v}$ and $\boldsymbol{v}_s$ are related as follows by introducing $\boldsymbol{s}$, which is the unit vector in the wheel driving direction:

$$\begin{aligned}\boldsymbol{v}\cdot\boldsymbol{s} &= \boldsymbol{v}_s\cdot\boldsymbol{s}+\boldsymbol{v}_f\cdot\boldsymbol{s}\\ &= \pm|\boldsymbol{v}_s||\boldsymbol{s}|+0=v_s. \quad \ldots\ldots\ldots \quad (3)\end{aligned}$$

Note that the sign of v_s is the direction of rotation. If we decide position $\boldsymbol{p}_i$ and orientation $\boldsymbol{s}_i$ of each wheel, we derive speed as follows:

$$v_{si} = (\boldsymbol{\omega}\times\boldsymbol{p}_i)\cdot\boldsymbol{s}_i. \quad \ldots\ldots\ldots\ldots \quad (4)$$

This is independent of the number of wheels, so more than three wheels may be used as needed to disperse a heavier load or for more stably support multiple ball contact (our minimum number of contact is three).

With wheels arranged as shown in **Figs. 3(b)** and **(c)**, with contacts at zenith angle ϕ and equally spaced on the horizontal plan, the point $\boldsymbol{p}_i$ is as follows:

$$\begin{aligned}\boldsymbol{p}_1 &= (r\sin\phi, 0, r\cos\phi)\\ \boldsymbol{p}_{2,3} &= (-\frac{1}{2}r\sin\phi, \pm\frac{\sqrt{3}}{2}r\sin\phi, r\cos\phi), \quad \ldots \quad (5)\end{aligned}$$

r is the ball radius. The drive direction $\boldsymbol{s}_i$ is determined as follows:

$$\begin{aligned}\boldsymbol{s}_1 &= (0,-1,0)\\ \boldsymbol{s}_{2,3} &= (\pm(\sqrt{3}/2),(1/2),0). \quad \ldots\ldots \quad (6)\end{aligned}$$

Wheel speed v_{si} is derived when the ball rotates around the x-axis at angular velocity ω_x, i.e., $\boldsymbol{\omega} = (\omega_x, 0, 0)$ as follows:

$$\begin{aligned}v_{s1} &= r\cos\phi\ \omega_x\\ v_{s2,3} &= -(1/2)r\cos\phi\ \omega_x. \quad \ldots\ldots\ldots \quad (7)\end{aligned}$$

Similarly, when $\boldsymbol{\omega} = (0, \omega_y, 0)$, derivation is as follows [4]:

$$\begin{aligned}v_{s1} &= 0\\ v_{s2,3} &= \pm(\sqrt{3}/2)r\cos\phi\ \omega_y. \quad \ldots\ldots\ldots \quad (8)\end{aligned}$$

These two components are independent, so we add them to get actual wheel speed for inverted pendulum control.

Lastly, rotation around the vertical axis using $\boldsymbol{\omega} = (0, 0, \omega_z)$ makes as follows:

$$v_{s1,2,3} = -r\sin\phi\ \omega_z. \quad \ldots\ldots\ldots\ldots \quad (9)$$

Virtual wheel command velocity (v_x, v_y) derived from acceleration as the control input is converted to the velocity of the three *real* wheels as follows:

$$\begin{aligned}v_{s1} &= -v_y\ \cos\phi + K_z\omega_z\\ v_{s2} &= \{+(\sqrt{3}/2)v_x + (1/2)v_y\}\cos\phi + K_z\omega_z\\ v_{s3} &= \{-(\sqrt{3}/2)v_x + (1/2)v_y\}\cos\phi + K_z\omega_z\ . \quad (10)\end{aligned}$$

$K_z = -r\sin\phi$ is a coefficient of turning (pivoting) around the vertical axis independent of inverted pendulum control.

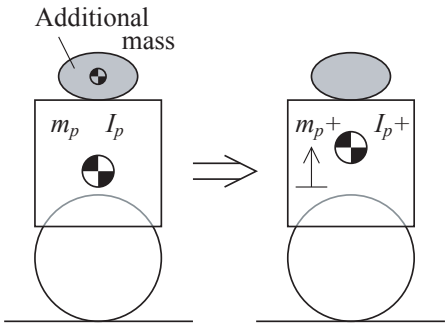

Fig. 6. Additional loading mass.

Zenith angle ϕ determines the ratio of wheel to ball rotation and affects the robot body support [4]. If $\phi = \pi/2$, for example, the ball cannot be driven in x and y directions while the ball rotates freely (even though if $\phi = \pi/2$, the ball can be driven if wheels are skewed). ϕ is also mechanically constrained so that wheels do not mutually interfere. Based on these considerations, we used 45° for our first prototype and 50° for its successors.

3.3. Acceleration Control Input to Inverted Pendulum

As stated below, using ball acceleration for input calculated by the control equation instead of torque to drive the ball made the robot rather robust against change of inertia.

The author Kumagai had built several inverted pendulums that used the actuator acceleration as the system inputs before this robot. The acceleration was used because it only requires a velocity/position controlled motor (not torque/current controlled), making the system simple and less expensive, and because the acceleration and the torque have a positive correlation (roughly proportional). This acceleration input method worked well enough although it had not been analyzed. We took the same approach because we used the stepping motors for our robot, which simplified the robot and low-backlash direct drive enables smooth movement. The completed robot, in fact, was strongly robust against the change in robot inertia parameters, causing us to analyze differences in the torque/force input and acceleration input.

Assuming that an object is loaded on the robot as shown in **Fig. 6**. Pendulum weight and inertia moment increase due to load weight, raising the center of mass. The inverted pendulum must resist overturning moment due to gravity *acceleration*. For torque input, robot acceleration generated by motors decreases almost inversely proportionately to inertia increase. Intuitively, however, inertia has less impact on output in acceleration input.

We used the Nyquist diagram for theoretical analysis. The robot is modeled on a vertical plane as shown in **Fig. 4**, with I_p, I_b, m_p, and m_b as inertia moment and mass of robot body (pendulum) and ball, r ball radius, h pendulum center of mass height, θ pendulum inclination, ψ

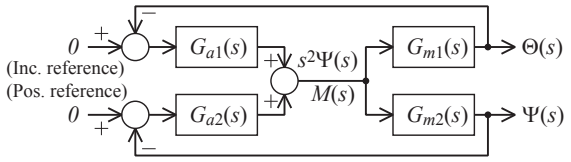

(a) Faithful to the control algorithm

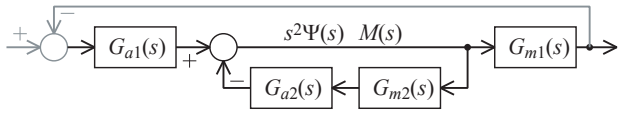

(b) Modified for open-loop transfer function

Fig. 7. System block diagram for analysis.

relative angle between the pendulum and ball (the driving angle of the ball by wheels), and M torque applied to the ball. Two sets of motion equations – two translations and one rotation for each – on the pendulum and ball are derived by introducing interaction M and horizontal and vertical forces, yielding three transfer functions using linearization and Laplace transformation [7]:

$$\frac{\Theta}{\Psi} = \frac{\{I_b + (m_p + m_b)r^2 + m_p hr\}s^2}{m_p hg - \{I_p + m_p(h+r)^2 + I_b + m_b r^2\}s^2} \quad (11)$$

$$\frac{\Theta}{M} = \frac{I_b + (m_p + m_b)r^2 + m_p hr}{\{m_p hg - As^2\}\{I_b + (m_p + m_b)r^2\}} \quad (12)$$

$$\frac{\Psi}{M} = \frac{m_p hg - \{I_p + m_p(h+r)^2 + I_b + m_b r^2\}s^2}{\{m_p hg - As^2\}\{I_b + (m_p + m_b)r^2\}s^2} \quad (13)$$

$$A = I_p + m_p h^2 \left(1 - \frac{1}{1 + (m_b/m_p) + (I_b/m_p r^2)}\right)$$

g is gravity acceleration and A a complex term substitution. The Eq. (11) is rewritten as follows:

$$\frac{\Theta}{s^2\Psi} = \frac{(I_b + (m_p + m_b)r^2 + m_p hr)}{m_p hg - \{I_p + m_p(h+r)^2 + I_b + m_b r^2\}s^2}, \quad (14)$$

meaning that system input is the ball's angular acceleration. The other equation is prepared in the same manner:

$$\frac{\Psi}{s^2\Psi} = \frac{1}{s^2}. \quad \ldots\ldots\ldots\ldots\ldots (15)$$

The robot control Eq. (1) is rewritten as PD feedback of pendulum inclination Θ and wheel rotation Ψ, as follows:

$$s^2\Psi_{inp} = K_1(1 + \tau_1 s)\Theta + K_2(1 + \tau_2 s)\Psi \quad \ldots (16)$$

$$M_{inp} = K_1(1 + \tau_1 s)\Theta + K_2(1 + \tau_2 s)\Psi, \quad \ldots (17)$$

Eq. (16) inputs angular wheel acceleration as we proposed and Eq. (17) inputs torque as is generally done, to compare them.

We derived the open-loop transfer function from **Fig. 7** control as follows:

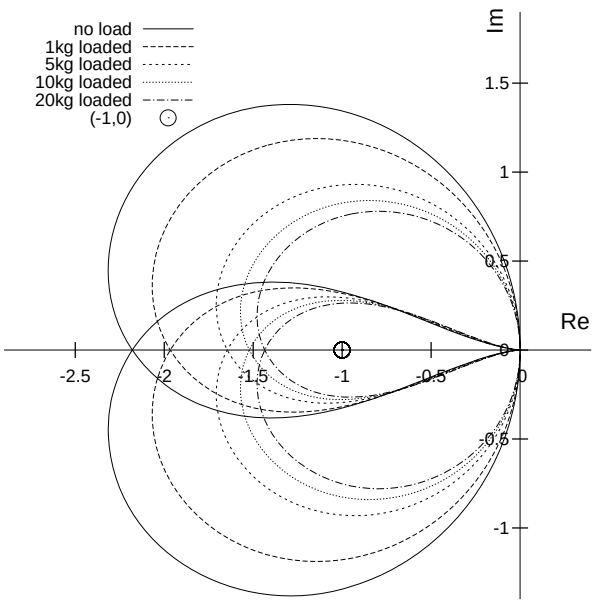

(a) Acceleration input

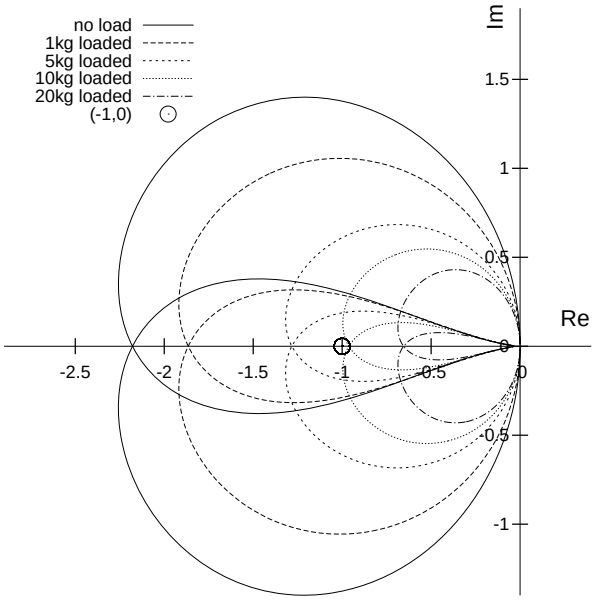

(b) Torque input

Fig. 8. Nyquist diagram of the robot with point mass loaded above the robot.

$$G(s) = \frac{G_{a_1} G_{m_1}}{1 + G_{a_2} G_{m_2}}$$

$$G_{a_1} = -K_1(1 + \tau_1 s), \quad G_{a_2} = -K_2(1 + \tau_2 s)$$

$$G_{m_1} = \frac{\Theta}{s^2\Psi} \text{ or } \frac{\Theta}{M}$$

$$G_{m_2} = \frac{\Psi}{s^2\Psi} \text{ or } \frac{\Psi}{M} \quad \ldots\ldots\ldots (18)$$

This yields the Nyquist diagrams in **Fig. 8**. $(K_1, \tau_1, K_2, \tau_2) = (196.9, 0.26, 1.9, 0.96)$ was used for acceleration input control gain, which were actual robot gains. $(K_1, \tau_1, K_2, \tau_2) = (21.1, 0.15, 0.035, 1.65)$

Table 2. Typical control gains.

Gain	linear acceleration	angular acceleration	(for Nyquist analysis)
K_A	378.1 (mm/s^2)/(°)	196.9 (rad/s^2)/(rad)	$K_1 =$ 196.9 (rad/s^2)/(rad)
K_{AV}	96.8 (mm/s^2)/(°/s)	50.4 (rad/s^2)/(rad/s)	$\tau_1 =$ 0.26 s
K_T	1.9 (mm/s^2)/(mm)	1.9 (rad/s^2)/(rad)	$K_2 =$ 1.9 (rad/s^2)/(rad)
K_V	1.8 (mm/s^2)/(mm/s)	1.8 (rad/s^2)/(rad/s)	$\tau_2 =$ 0.96 s

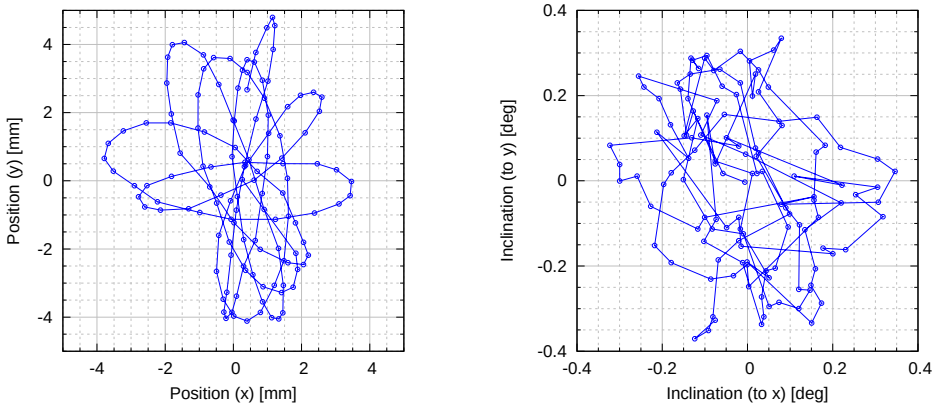

(a) Position [mm] (b) Inclination [deg]

Fig. 9. Experimental fluctuation when robot was commanded to remain stationary. The acquisition interval (graph points) was 50 ms.

was used for the torque control model, chosen so that Nyquist diagrams of both controls roughly coincide when additional mass is not loaded on the robot, and robot parameters in **Table 1** are used. Results were calculated assuming the robot had no additional mass or 1, 5, 10, or 20 kg of load. Stability is maintained if the dual-loop diagram intersection is to the left of $(-1,0)$, but not if it is to the right, because transfer functions have two poles to the right of the imaginary axis and the plot must encircle the point twice to ensure stability.

Both intersections move to the right but in different trends. The intersection moves across critical point $(-1,0)$ in the torque-input model, although apparently converging at a point to the left of the critical point in acceleration-input. When we load 10 kg on the robot, acceleration input changed little but would have failed for torque input. Larger gains can rightly improve the load limitation in torque-input but too large gains usually cause problems on the actual system.

Using acceleration (velocity) controlled in ball driving has another advantage. In case one of the torque-commanded wheels detach from the ball, it spins up, which will not occur in the acceleration-commanded wheel because its velocity is decided whether it touch the ball. This is helpful for an over-constrained case of a robot with more than three wheels. We need only to calculate the wheel speed using the position and the direction of each wheel. The only disadvantage is that we cannot keep the robot leaned from the vertical line without its move whereas the torque-input control can do only with a side-effect that it generates some propelling force. The control fails if we rigidly connect several acceleration-controlled robots, whose both relative position and attitude are constrained.

4. Experiments

We tuned the robot's parameters experimentally, and typical gains are in **Table 2**. Gain sets labeled linear and angular acceleration are identical but units differ. The left set of gains is in intuitive units used in the following results. The set in angular units with remarks is in radians for previous analysis. Both are converted from the gains used for the actual robot control because it used fixed point calculations in specific units (just for reference, the four gains were (1500, 600, 50, 600)).

The robot was made to remain stationary on a flat floor as shown in **Fig. 9**. Results indicate deviation in the steady state. The robot stayed within 10 mm range. Note that position was calculated from the wheel rotation command, and differs in detail from that in actual movement.

Results for when the robot was commanded to move straight at approximately 100 mm/s and 600 mm/s along the y-axis are shown in **Fig. 10**. At lower speed, less fluctuation occurred in inclination and fewer positioning errors than at higher speed. Undershoot observed when the robot started moving occurred in both speeds due to inverted pendulum itself. The robot must lean in the direction of movement to accelerate, so to do so, it kicked the ball back, initiating robot fluctuation causing large overshoot at higher speed – actual maximum speed was almost 1100 mm/s. This indicates the need to optimize undershoot and overshoot, i.e., acceleration and deceleration. Positioning error along the x-axis (no movement commanded) in **Fig. 10** appears to due to coupling of movement and control on the two axes. In other experiments, the robot could rotate through 60°/s.

In carrier experiments in **Fig. 11**, the robot remained stable carrying a 10 kg-concrete block using the same

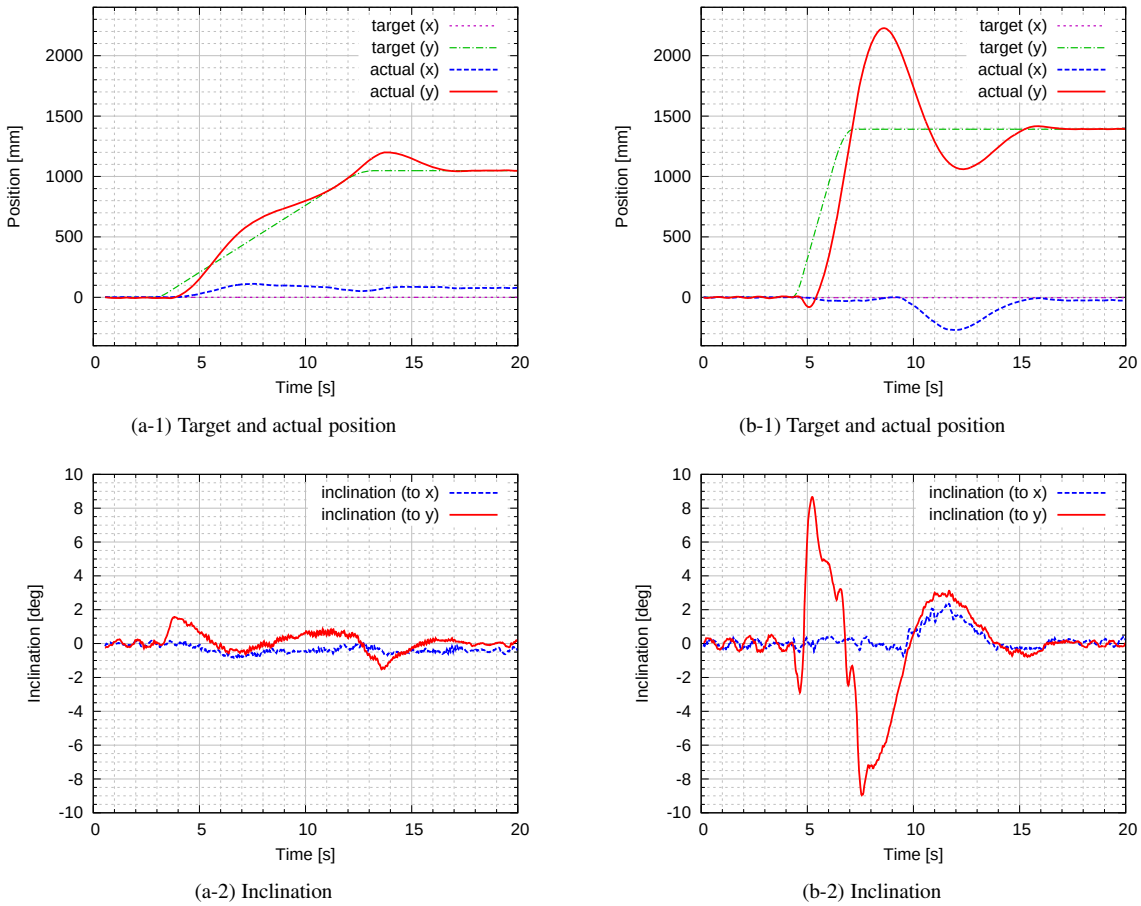

(a-1) Target and actual position

(b-1) Target and actual position

(a-2) Inclination

(b-2) Inclination

Response for commanded velocity of 110 mm/s.

Response for commanded velocity of 620 mm/s.

Fig. 10. Experimental changes in target and actual position and inclination when the robot was commanded to move straight.

(a) Load the robot with concrete block and move it with a finger.

(b) Human-robot cooperation.

Fig. 11. Robot transport.

control gains as in **Fig. 11(a)**. In control Eq. (1), gain K_T maintains robot position. The robot is moved easily by cutting K_T to zero, with the gain K_V acting as a brake and K_A and K_{AV} maintain robot attitude. The robot was led easily in any direction using minimal force. This carrier-mode can naturally cooperate with human or other robots as shown in **Fig. 11(b)** without any force sensors and a specific control scheme. A ball joint was used to decouple the load attitude, which is important to avoid the disadvantage of acceleration-input.

5. Conclusions

We have developed a robot that rides and balances on a ball, traversing and pivoting on its vertical axis.

The robot used acceleration as control input, unlike most inverted pendulums which use actuator torque or force. The advantage of using acceleration in robustness was confirmed. The method is applicable to stepping motors and industrial motors with speed/position input controllers. Acceleration-input discussed for inverted pendulum control is also potentially applicable in often

uses of force/torque, e.g., suppressing vibration, where force/torque is not essentially required.

The robot fluctuated little in steady state, and could carry a load heavier than itself with no change in gain. Its movement is easily guided by small external force when one of the gains is cut.

We plan to improve the robot as a carrier and to use multiple robots cooperatively in second report.

Acknowledgements

We thank RIKEN, the patent administrator, and wheel's inventors for letting us use the omnidirectional wheel and are indebted to the engineers at the Tohoku Gakuin University workshop for making most of the mechanical parts used in this research.

References:

[1] M. Kumagai, T. Ochiai, and N. Konno, "Development of Inverted Pendulums that Move on Floor – Balancing Robot on a Ball and Hopping Robot using a Linear Motor –," Proc. Robomec08, 2P1-C11, 2008.
[2] M. Kumagai and T. Ochiai, "Cooperative Transport using Robots Balanced on Balls," Proc. Robomec09, 2P1-D18, 2009.
[3] M. Kumagai and T. Ochiai, "Development of a Robot Balancing on a Ball," Proc. ICCAS 2008, pp. 433-438, 2008.
[4] M. Kumagai, and T. Ochiai, "Development of a robot balanced on a ball – Application of passive motion to transport –," Proc. ICRA 2009, pp. 4106-4111, 2009.
[5] H. G. Nguyen, J. Morrell, K. Mullens, A. Burmeister, S. Miles, N. Farrington, K. Thomas, and D. Gage, "Segway robotic mobility platform," SPIE Proc. 5609: Mobile Robots XVII, pp. 207-220, 2004.
[6] Y. Hosoda, S. Egawa, J. Tamamoto, K. Yamamoto, R. Nakamura, and M. Togami, "Development of Human-Symbiotic Robot "EMIEW" – Design Concept and System Construction –," J. of Robotics and Mechatronics, Vol.18, No.2, pp. 195-202, 2006.
[7] T. Emura and T. Sakai, "Study on Inverted Pendulum that Maintains Erect Position using Reaction Wheel," Biomechanism, pp. 321-328, 1973 (in Japanese, available at CiNii, NAID:110004695233).
[8] T. B. Lauwers, G. A. Kantor, and R. L. Hollis, "A Dynamically Stable Single-Wheeled Mobile Robot with Inverse Mouse-Ball Drive," Proc. ICRA 2006, pp. 2884-2889, 2006.
[9] U. Nagarajan, M. Anish Mampetta, G. Kantor, and R. Hollis, "State Transition, Balancing, Station Keeping, and Yaw Control for a Dynamically Stable Single Spherical Wheel Mobile Robot," Proc. ICRA 2009, pp. 998-1003, 2009.
[10] T. Endo and Y. Nakamura, "An Omnidirectional Vehicle on a Basketball," Proc. ICAR'05, pp. 573-578, 2005.
[11] D. Chugo, K. Kawabata, H. Kaetsu, H. Asama, and T. Mishima, "Development of Omni-directional Vehicle with Step-Climbing Ability," Proc. ICRA 2003, pp. 3849-3854, 2003.
[12] H. Asama, H. Kaetsu, I. Endo, and M. Sato, "Wheel for Omnidirectional Mobile Robot," JP-patent No.3421290, 2003.
[13] N. Hiraoka and T. Noritsugu, "Sliding Mode Posture Control of a Parallel Biwheel Vehicle Driven with Stepping Motor," Trans. of the JSME. C, Vol.62, No.601, pp. 3580-3587, 1996.
[14] N. Hiraoka and T. Noritsugu, "Reaction Force Control of a Parallel Biwheel Vehicle Driven with a Stepping Motor," J. of Robotics and Mechatronics, Vol.11, No.5, pp. 356-361, 1999.
[15] T. Emura, M. Kumagai, and K. Ogawa, "Expansion of Frequency Response Using Multiple Sensors and Subtraction Type of Filter," Proc. Machatronics Vol.96, No.2, pp. 197-202, 1996.
[16] C. Y. Chung, J. W. Lee, S. M. Lee, and B. H. Lee, "Balancing of an Inverted Pendulum with a Redundant Direct-Drive Robot," Proc. ICRA 2000, pp. 3952-3957, 2000.

Name:
Masaaki Kumagai

Affiliation:
Associate Professor, Faculty of Engineering, Tohoku Gakuin University

Address:
1-13-1 Chuo, Tagajo, Miyagi 985-8537, Japan

Brief Biographical History:
2000- Research Associate, Tohoku University
2003- Lecture, Tohoku Gakuin University
2006- Associate Professor
2009-2010 Visiting Professor, The Robotics Institute, Carnegie Mellon University (concurrently)

Main Works:
• "Wheel Locomotion of a Biped Robot Using Passive Rollers," Masaaki Kumagai and Kaoru Tamada, J. of Robotics and Mechatronics, Vol.20, No.2, pp. 206-212, 2008.

Membership in Academic Societies:
• The Japan Society of Mechanical Engineers, Robotics and Mechatronics Division (JSME, RMD)
• The Society of Instrument and Control Engineers (SICE)
• The Robotics Society of Japan (RSJ)
• The Institute of Electrical and Electronics Engineers (IEEE)

Name:
Takaya Ochiai

Affiliation:
Graduate School of Tohoku Gakuin University

Address:
1-13-1 Chuo, Tagajo, Miyagi 985-8537, Japan

Brief Biographical History:
2008- Master's Course, Graduate School of Tohoku Gakuin University
2010- Tohoku Ricoh Co., Ltd.

Main Works:
• "A Study on Traveling over a Bump of a Robot Balanced on a Ball," Takaya Ochiai and Masaaki Kumagai, Research workshop of SICE Tohoku chapter, 254-3, Dec. 2009.

Membership in Academic Societies:
• The Society of Instrument and Control Engineers (SICE)